Ultrafast single photon emitting quantum photonic structures based on a nano-obelisk

Je-Hyung Kim, Young-Ho Ko, Su-Hyun Gong, Suk-Min Ko, Yong-Hoon Cho[*]

Department of Physics, Graduate School of Nanoscience & Technology (WCU), and KAIST Institute for the NanoCentury, KAIST, Daejeon, 305-701, Republic of Korea

I. Formation of GaN nanostructures by chemical vapor-phase etching and improvement of structural and optical properties

The chemical vapor-phase etching method using HCl gas at high temperature has many advantages with respect to control of GaN. Contrary to the chemical wet etching method, which is difficult to etch GaN due to its strong chemical stability, especially Ga-polar GaN, the chemical vapor-phase etching can effectively etch Ga-polar GaN and form high-quality nanostructures on a large area (Fig. S1a). The shapes of nanostructures can be controlled by a facet-selective etching mechanism. Fig. S1b is a TEM image for the early stage of the chemical vapor-phase etching process, and show that dislocations are terminated between nanostructures. Since defect regions have poor crystal quality, they are eliminated more rapidly than the high-crystal regions. Therefore, the remaining nanostructures have high crystal quality. This structural property improves the optical property of the nanostructure. Figure S1c shows macro PL spectra at 10 K. Compared to the GaN epilayer (before etching), the as-etched GaN nanostructure shows a large increase in PL intensity about ten times and a narrow FWHM of GaN near a band edge emission at around 3.47 eV. This improved optical property is induced by increased light extraction efficiency and reduction of defects in nanostructures. By the formation of nanostructures, the residual strain is also reduced, and this results in a peak shift toward lower energy of 13 meV for the nanostructures in Fig. S1c. Details of the chemical vapor-phase etching method and characterization can be found in our previous work[1].

[*] Electronic address: yhc@kaist.ac.kr

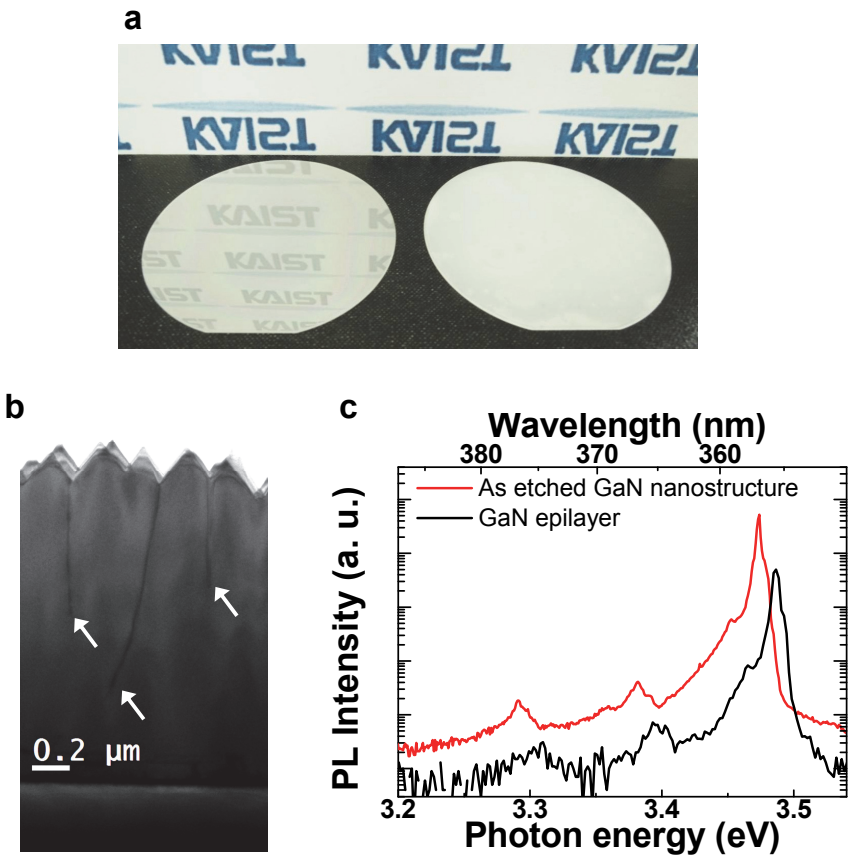

Figure S1. Formation of high quality GaN nanostructures. a, Photographic image for GaN film (left) and as-etched GaN nanostructures (right). **b**, Cross-sectional TEM image after a chemical vapor-phase etching process. White arrows indicate dislocations. **c**, PL spectra for the as-etched GaN nanostructure (red) and GaN epilayer (black) at 10 K.

II. Light extraction efficiency in nano-obelisks

Light extraction is an important factor for optical devices and is influenced by the structure geometry. In the boundary between high index materials and low index air, total internal reflection occurs and this reflection is severe in a planar structure. Many approaches to increase light extraction efficiency have been developed such as surface roughening[2], patterned substrates[3], and photonic crystal structures[4]. The formation of nanostructures is an effective approach, especially when coupled with a tapered structure[5-7]. To estimate the light extraction efficiency of our GaN nano-obelisk structure with a diameter of 200 nm and a sharp pyramidal tip, we simulated the light extraction efficiency by solving Maxwell's equation using the 3-dimensional finite-difference time-domain method (Lumerical Solutions) and compared the results with those of pillar-type nanostructures with a flat top surface and planar structures. Single dipoles were situated at the positions of QDs. Figure S2 shows the light extraction efficiency of each structure, which was obtained by the ratio of the emitted power toward top surface (air) to the total emitted power. The planar structure shows only 4 % light extraction efficiency toward the top surface (air), and most of the emission is reflected backward. Meanwhile, the nanostructures show substantially improved light extraction efficiency of about 20 % and 36 % for the pillar-type nanostructure and the nano-obelisk structure, respectively for the wavelength at 400 nm. In this simulation, we assume the nanostructures are standing on the GaN substrate. Therefore, more than half percent of the emission escapes toward the back side. Recently, near-unity light extraction efficiency of 97 % was achieved using tailored photonic nanostructures by transferring the nanostructures onto a metal film[5]. The possibility of transfer is one of the advantages of employing nanostructures.

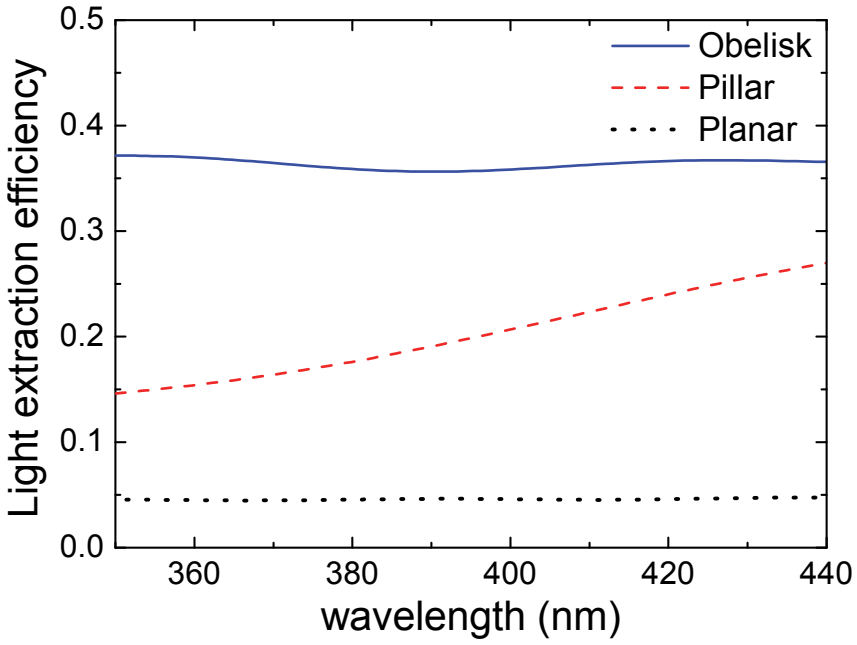

Figure S2. Comparison of light extraction efficiency for different structures. Light extraction efficiency toward upside are shown in the wavelength around 400 nm for the obelisk-shaped nanostructures with a pyramidal tip (blue line), pillar-type nanostructures with a flat end (red dashed line), and planar epilayer (black dotted line).

III. InGaN QW regrowth on etched GaN nanostructures

Based on high-quality GaN nanostructures formed by chemical vapor-phase etching, we grew InGaN QW and GaN barriers using MOCVD. Figure S3a-c shows scanning electron microscope (SEM) images of as-etched GaN nanostructures (Fig. S3a), thick obelisk-shaped GaN nanostructures including 3-period InGaN multi-QWs (Fig. S3b) and thin obelisk-shaped GaN nanostructures including a single QW (Fig. S3c). During the regrowth process, radial growth occurs more dominantly than axial growth, resulting in a GaN/InGaN core-shell structure.

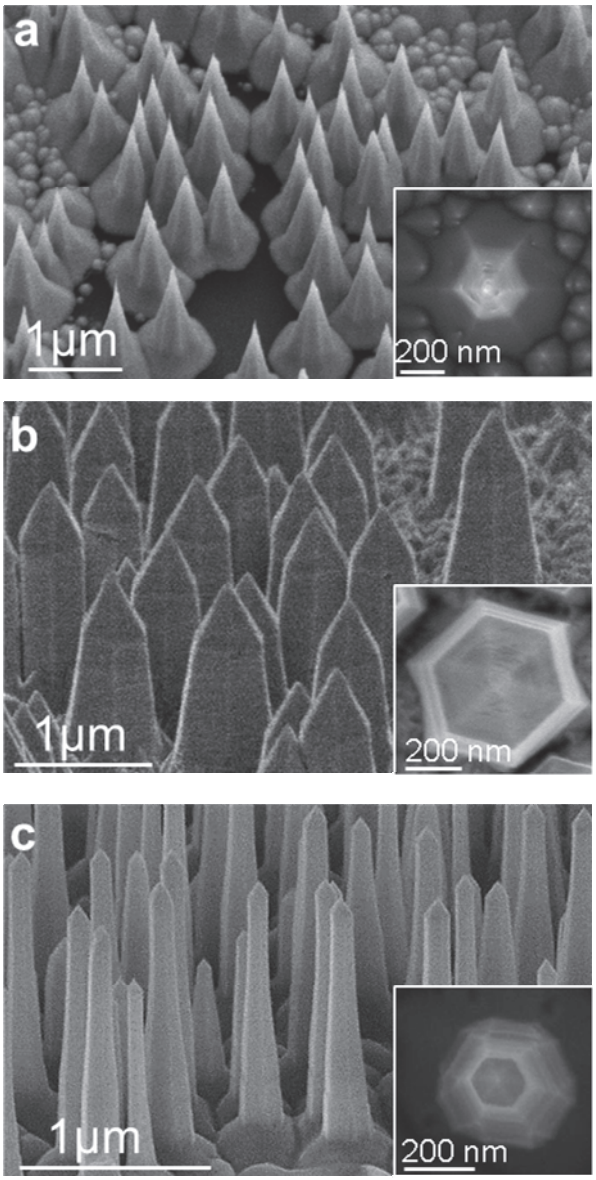

Figure S3. Obelisk-shaped GaN nanostructures including InGaN quantum structures. a-c, Tilted view SEM images for as-etched GaN nanostructures (**a**), GaN nanostructures including 3 periods InGaN QWs (**b**), and GaN nanostructures including a single InGaN QW (**c**). Insets show a top-view SEM image of each nanostructure.

IV. Nano-obelisks with multiple-InGaN QWs

In order to study InGaN QWs in nano-obelisks, we grew 3-period InGaN QWs with QW growth time of 100 s, 300 s, and 900 s at 680 ºC (Fig. S4a). The thicknesses of the InGaN QWs in the nano-obelisk were about 1.5 nm (inside), 5 nm (middle), and 17 nm (outside), respectively, at the column part (Fig. S4b5). The thickness of the QWs drastically decreased at the pyramidal tip part by less than half of that in the column part due to the different growth rate between two different facets[8,9] (Fig. S4b2-b4). Interestingly, the formation of an InGaN island was observed at the top of the pyramid tip (Fig. S4b1,c). This result motivated us to form a well-isolated small island (QD) at the top of the nano-obelisk by growing a thin QW, as seen in Fig. 2 of the manuscript.

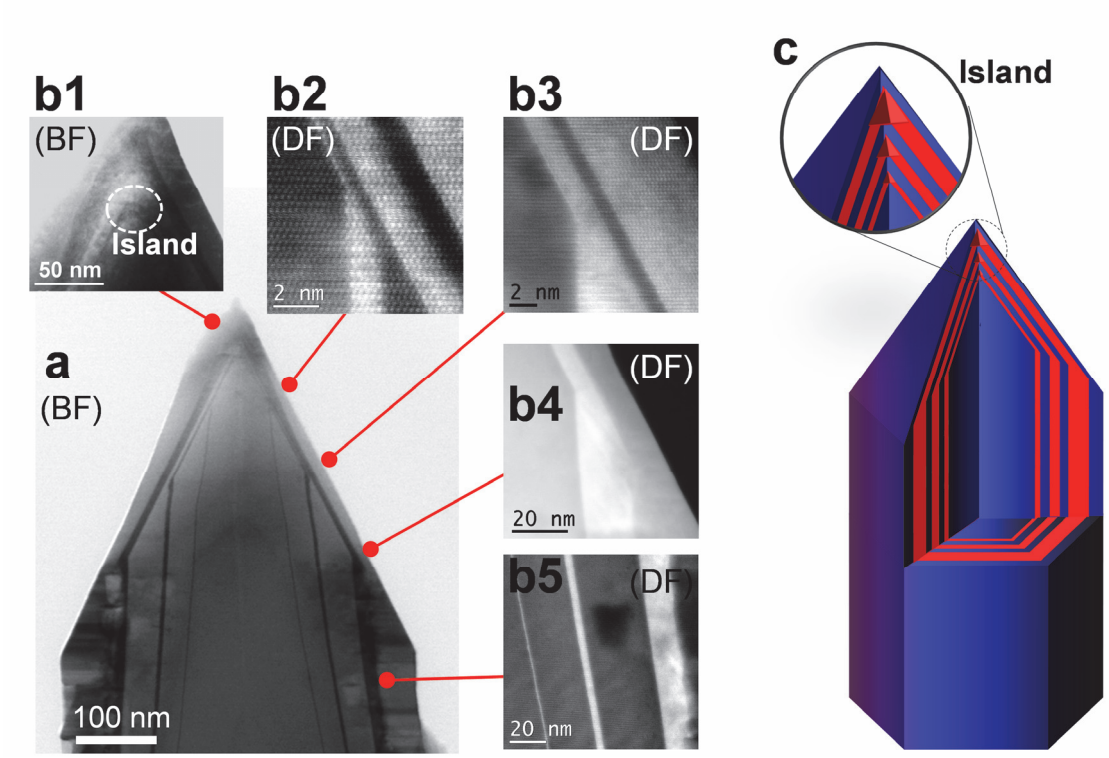

Figure S4. Structural properties of the 3-period InGaN QW in a GaN nano-obelisk. a,**b1-b5**, Cross-sectional STEM bright-field (**b1**) and dark-field images (**b2-b5**). GaN nano-obelisk including 3 periods InGaN QWs with different well thickness of 1.5 nm (inside), 7 nm (middle) and 15 nm (outside) at column part (**b5**). **b2-b4** show a reduction of QW thickness at the pyramidal facet compared to the column facet. **b1**, An island is formed at the top of the pyramidal tip. STEM images in (**a,b1**) are measured at bright field condition (dark region is InGaN) and (**b2-b5**) were measured at dark field condition (bright region is InGaN) **c**, Schematic illustration of GaN nano-obelisk including 3-period InGaN QWs.

V. Built-in field reduction and fast recombination time in multiple InGaN QWs on nano-obelisks

The optical properties of nano-obelisk ensembles with multipl-InGaN QWs in Fig. S4 were studied in a macro-PL system at 15 K with a 340 nm Ti:sapphire pulse laser (200 fs). Figure S5a shows a PL spectrum of InGaN QWs on nano-obelisks. InGaN QWs show two peaks at 425 nm and 470 nm. We surmise that the higher energy peak is from the 1.5 nm-thick QW, which has similar wavelength with that of the SQW-NO, and the lower energy peak is from the 5 nm- and 17 nm-thick QWs. Because we grew three QWs of the MQW-NO sample at the same growth conditions except for the growth time, the emission wavelength shift between the QWs is attributed mostly to the quantum confinement effect[10]. The indium composition was analyzed by an energy-dispersive x-ray microanalysis, and it was around 20 % for the 5 nm thick-QW.

Generally, strained InGaN QWs embedded in a planar structure has a poor radiative recombination efficiency due to the existence of a built-in electric field. However the nano-obelisk effectively eliminate the built-in field and show very high radiative recombination efficiency, which results in unusual single exciton properties and ultrafast recombination in the manuscript (Fig. 3 and 4). Similar to thin single QW and QD, Multiple-QWs in the nano-obelisk show fast recombination time regardless of thickness. Figures S5b shows decay curves of InGaN QWs on nano-obelisks at the wavelength of 470 nm and 420 nm and their recombination values are 94 ps and 166 ps, respectively. A 2 nm-thick InGaN QW grown on a planar structure is also compared at the wavelength of 470 nm, which shows conventional long recombination time of 1.18 ns. This result indicates that InGaN QWs embedded in the nano-obelisk have a fast recombination time even in thick QWs thickness due to the reduced built-in field.

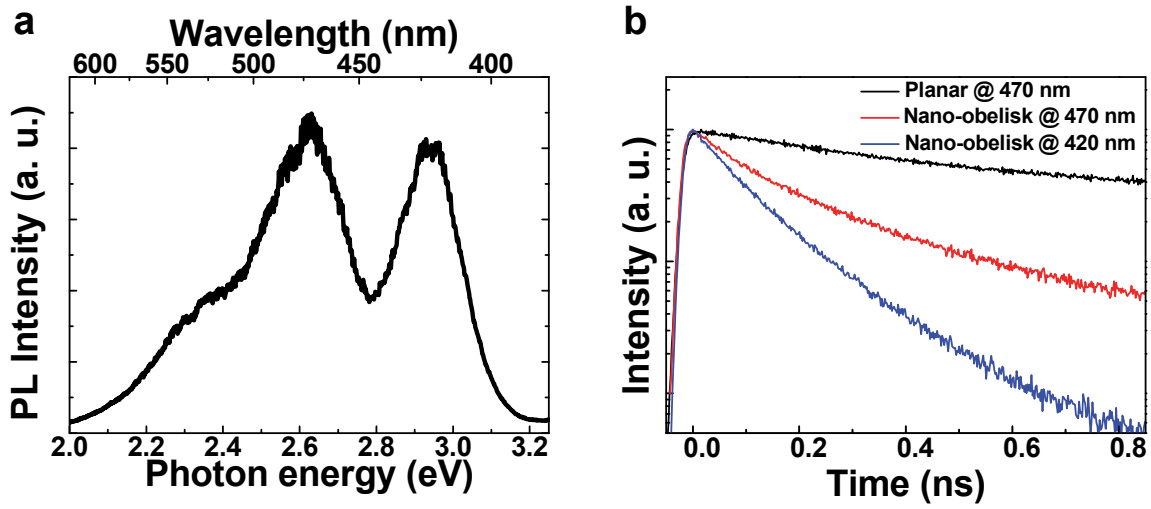

Figure S5. Optical study for ensemble of nano-obelisks and a planar QW sample. a, Time-integrated macro-PL spectra of multiple-InGaN QWs embedded in nano-obelisks at 15 K. **b**, Comparison of decay curves for InGaN QWs grown on a planar structure at peak position of 470 nm and InGaN QWs embedded in nano-obelisks at peak position of 470 nm and 420 nm.

VI. Temperature dependent TRPL

The single InGaN QW formed in the SQW-Planar and SQW-NO samples show a significant difference in the PL intensity, peak position, lifetime, and so on (Fig. S6). In particular, the reduction of the built-in electric field results in the unusual fast decay time in the nano-obelisk. To investigate the influence of the nonradiative process in the nano-obelisks, we performed temperature dependent PL experiments. Generally, the nonradiative process is restricted at low temperature, whereas with increasing temperature, the nonradiative recombination rate increases rapidly and causes quenching of the PL emission at high temperature. In both samples, the PL intensity decreases with increasing temperature by involving the nonradiative process (Fig. S6a1,b1). This nonradiative process also induces decay time shortening with increasing temperature (Fig. S6a2,b2). However, different trends are observed for the two samples. For the SQW-Planar on the *c*-plane, the PL intensity and the decay time rapidly reduced with increasing temperature (Fig. S6a3), while for the SQW-NO, the PL intensity and the decay time remained at almost the same levels up to 100 K and started to decrease beyond 100 K (Fig. S6b3). This indicates that the nano-obelisks are less influenced by the nonradiative process at low temperature compared to the InGaN QW on the *c*-plane due to the reduction of defects and the negligible built-in field in the nano-obelisk. Therefore, we conclude that the observed fast recombination time of the nano-obelisk at low temperature is dominated by the fast radiative recombination process.

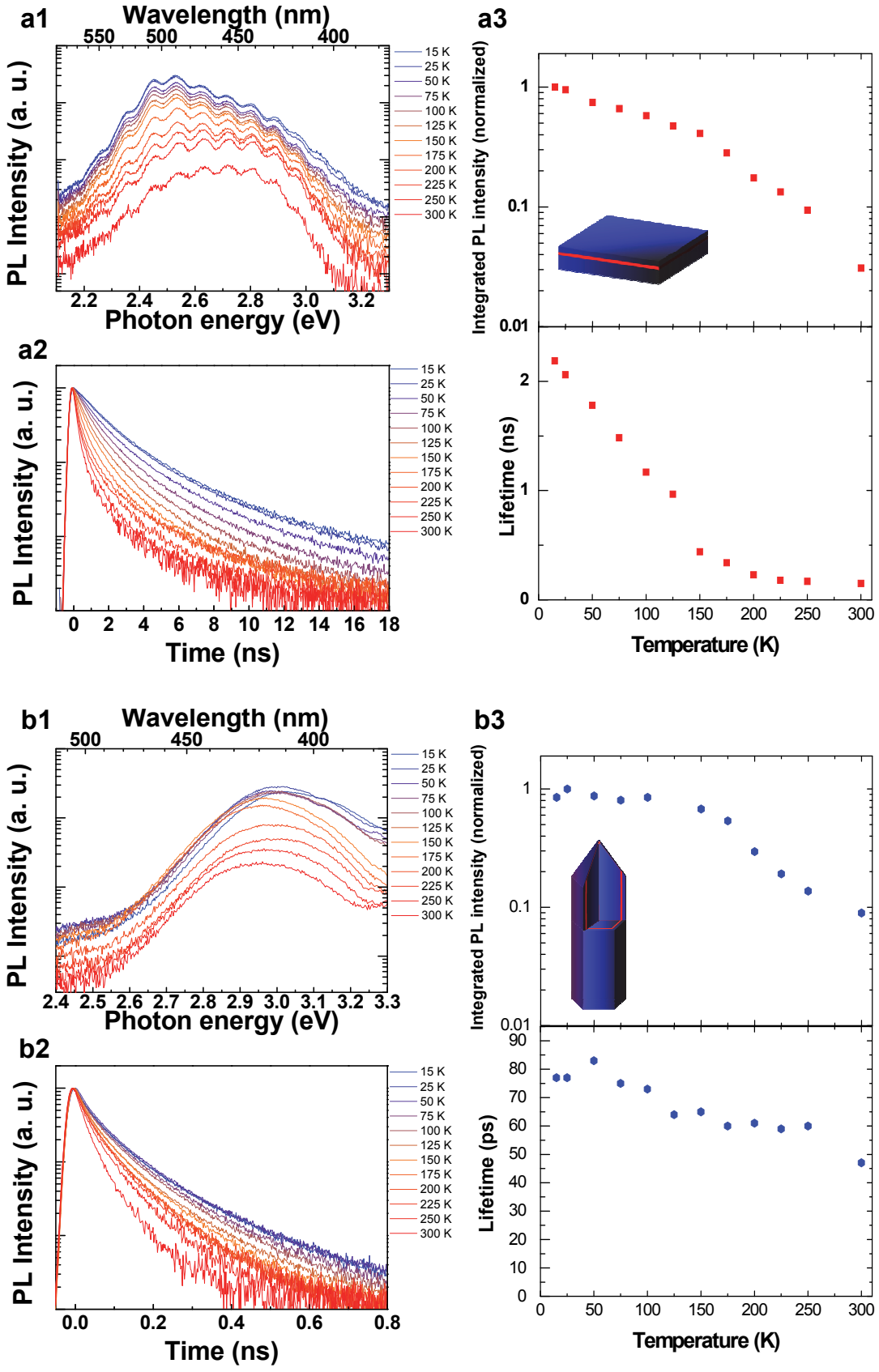

Figure S6. Temperature dependent time-integrated and -resolved PL. a1,**b1** Time integrated PL spectra depending on temperature from 15 K to 300 K for the SQW-Planar (**a1**) and SQW-NO (**b1**). **a2**, **b2**, Time-resolved PL decay curves with increasing temperature for the SQW-Planar (**a2**) and SQW-NO (**b2**). **a3**,**b3**, Integrated PL intensity and measured lifetime depending on temperature for the SQW-Planar (**a3**) and SQW-NO (**b3**).

References

1. Kim, J. H. *et al.* Dislocation-eliminating chemical control method for high-efficiency GaN-based light emitting nanostructures. *Cryst. Growth Des.* **12**, 1292-1298 (2012).
2. Schnitzer, I., Yablonovitch, E., Caneau, C., Gmitter, T. J. & Scherer, A. 30% external quantum efficiency from surface textured, thin-film light-emitting diodes. *Appl. Phys. Lett.* **63**, 2174-2176 (1993).
3. Gao, H. *et al.* Enhancement of the light output power of InGaN/GaN light-emitting diodes grown on pyramidal patterned sapphire substrates in the micro- and nanoscale. *J. Appl. Phys.* **103**, 014314-014315 (2008).
4. Boroditsky, M. *et al.* Light extraction from optically pumped light-emitting diode by thin-slab photonic crystals. *Appl. Phys. Lett.* **75**, 1036-1038 (1999).
5. Reimer, M. E. *et al.* Bright single-photon sources in bottom-up tailored nanowires. *Nat. Commun.* **3**, 737 (2012).
6. Babinec, T. M. *et al.* A diamond nanowire single-photon source. *Nat. Nanotech.* **5**, 195-199 (2010).
7. Claudon, J. *et al.* A highly efficient single-photon source based on a quantum dot in a photonic nanowire. *Nat. Photon.* **4**, 174-177 (2010).
8. Yeh, T. W. *et al.* InGaN/GaN multiple quantum wells grown on nonpolar facets of vertical GaN nanorod arrays. *Nano Lett.* **12**, 3257-3262 (2012).
9. Hong, Y. J. *et al.* Visible‐color‐tunable light‐emitting diodes. *Adv. Mater.* **23**, 3284-3288 (2011).
10. Grandjean, N. & Massies, J. GaN/AlGaN quantum wells grown by molecular beam epitaxy with thickness control at the monolayer scale. *Appl. Phys. Lett.* **73**, 1260 (1998).